Research Article

Jianye Zhang, Zhiyong Huang, Chengen He, Jinlong Zhang, Peng Mei, Xiaoyan Han*, Xianggang Wang, and Yingkui Yang*

Binary carbon-based additives in $LiFePO_4$ cathode with favorable lithium storage

https://doi.org/10.1515/ntrev-2020-0071
received August 20, 2020; accepted September 09, 2020

Abstract: A pairwise coupling of 0D Super-P (SP), 1D carbon nanotubes (CNTs), and 2D graphene nanosheets (GNs) into binary carbon-based conductive additives was used here for the $LiFePO_4$ cathode in lithium-ion batteries. For comparison, the $LiFePO_4$ cathode with SP, CNT, or GN unitary conductive agent was also examined. Electrochemical test results suggest that the cathodes with binary conducting additives present greatly improved electrochemical performance than the traditional cathode system (only SP used). Especially, the $LiFePO_4$ cathode containing 3% CNT component exhibits the highest specific capacity and the best cycling stability among all the cathodes with binary conducting additives, indicating that an appropriate amount of CNTs is critical in enhancing the conductivity and practical capacity output. However, an excess of CNTs leads to entangling with each other, hampering the uniform distribution of active materials and resulting in poor electrode performance. Furthermore, the combination of CNT and GN can effectively improve the capacity and cycling stability of the $LiFePO_4$ cathodes due to the synergistic effect of 3D conductive networks constructed by the two.

Keywords: binary conductive agents, graphene, carbon nanotubes, Super-P, lithium iron phosphate, lithium-ion batteries

1 Introduction

Recently, intensive research has been devoted to devising high-performance lithium-ion batteries (LIBs) by developing novel battery materials and designing innovative internal battery structure [1–10]. Practically, the electrochemical performance of LIBs mainly depends on the electrodes (cathode and anode), which are the key components of battery. In general, the electrodes are mainly comprised of active materials, conductive agents, and polymeric binders.

For the cathode materials, olivine-type lithium iron phosphate ($LiFePO_4$) has been intensively investigated due to its low cost, safety, and environmental friendliness [11–20]. However, it is difficult to attain the full theoretical capacity (170 mA h g^{-1}) because of its poor electronic conductivity (about 10^{-9} S cm^{-1}) [21–25] and low Li-ion diffusion coefficient (about 10^{-14}–10^{-16} cm^2 s^{-1}) [26–28]. Additionally, the common polymeric binder is an insulator by nature, which obstructs the electron transfer inside and between active materials and current collectors. Therefore, the conductive agent plays an important role in storing Li^+ by providing reinforced conductive network within the electrode to allow the active materials to perform effectively in the

* **Corresponding author: Xiaoyan Han,** Key Laboratory of Catalysis and Energy Materials Chemistry of Ministry of Education & Hubei Key Laboratory of Catalysis and Materials Science, South-Central University for Nationalities, Wuhan 430074, China, e-mail: xyhan@scuec.edu.cn
* **Corresponding author: Yingkui Yang,** Key Laboratory of Catalysis and Energy Materials Chemistry of Ministry of Education & Hubei Key Laboratory of Catalysis and Materials Science, South-Central University for Nationalities, Wuhan 430074, China; Hubei Engineering Technology Research Centre of Energy Polymer Materials, School of Chemistry and Materials Science, South-Central University for Nationalities, Wuhan 430074, China; Graphene R&D Center, Guangdong Xigu Tanyuan New Materials Corporation Limited & South-Central University for Nationalities, Foshan 528000, China, e-mail: ykyang@mail.scuec.edu.cn
Jianye Zhang: Key Laboratory of Catalysis and Energy Materials Chemistry of Ministry of Education & Hubei Key Laboratory of Catalysis and Materials Science, South-Central University for Nationalities, Wuhan 430074, China
Zhiyong Huang, Peng Mei: Hubei Engineering Technology Research Centre of Energy Polymer Materials, School of Chemistry and Materials Science, South-Central University for Nationalities, Wuhan 430074, China
Chengen He, Jinlong Zhang, Xianggang Wang: Graphene R&D Center, Guangdong Xigu Tanyuan New Materials Corporation Limited & South-Central University for Nationalities, Foshan 528000, China

cathode system. And the mechanism for enhancing the electrical conductivity of the electrodes is based on forming conduction bridges among active material particles. In this regard, a range of carbon materials such as carbon black (Super-P, SP), conducting graphite, and acetylene black are commonly adopted as the conductive agents to increase the capacity, rate capability, and cycling performance of the cathode system [29–39].

Nowadays, to effectively utilize the active materials, the proportions of the conductive carbon in the $LiFePO_4$ cathode system often reach up to about 3–5 wt% and even as high as 6–10 wt% especially in the case of high-rate LIBs. This substantially reduces the energy and power densities of the resulting batteries. Therefore, it is imperative to develop high-efficiency conductive agents that can afford adequate conducting network with appropriate addition amount for future high-performance LIBs.

The normally used conductive additives often display relatively low conducting efficiency due to their small particle surfaces (only the outer carbon plane can contact with active materials), which can be improved by introducing carbon materials with large specific surface area. Recently, graphene (GN) and carbon nanotubes (CNTs), as novel but powerful conductive additives, have attracted increasing attention because of their unique nanostructure, flexible conducting network, and excellent electronic conductivity. Due to its one-atom thick-layered 2D structure, graphene has large specific surface area, which can effectively establish contact with the active materials and favor fast Li^+ transport [40–46]. On the other hand, CNTs with wire-like shape and high aspect ratio are conductive to constructing continuous conductive network for rapid electron transfer [47–51]. Thus, the combination of CNTs with GN as composite conductive additives is supposed to construct a 3D structure that may form well-distributed conductive network to improve the electrochemical performance of the $LiFePO_4$ cathode. Up to now, there are few reports on the synergistic effect of GN and CNTs on the $LiFePO_4$ cathode.

Herein, we fabricated a series of binary carbon-based conductive additives consisting of SP, CNTs, and/or GN and investigated their impacts on the electrochemical performance of the $LiFePO_4$ cathodes. The electrochemical performances of the $LiFePO_4$ cathodes with single conductive agent (SP, GN, or CNTs) were also tested for comparison. This work will provide theoretical and practical bases for the application of high-performance conductive agents in LIBs.

2 Experimental

2.1 Materials

$LiFePO_4$ was purchased from BTR New Material Group Co. Ltd (China). SP was purchased from Timcal (Switzerland). CNTs and graphene were obtained from Chengdu Institute of Organic Chemistry, Chinese Academy of Sciences, and Guangdong Xigu Tanyuan New Materials Co. Ltd (China). Poly(vinylidene fluoride) (PVDF) and *N*-methyl-2-pyrrolidone (NMP) were purchased from Arkema (Changshu, China) and Sinopharm Chemical Reagent Co. Ltd (China), respectively. All chemicals were of analytical grade and used as received without further purification.

2.2 Electrode preparation

The $LiFePO_4$ cathode slurry with unitary and binary conductive agents was prepared via a facile mechanical stirring method. Typically, the preparation process of $LiFePO_4$ cathode slurry was performed in an agitated autoclave. First, 8 wt% dispersion liquid of PVDF in NMP was prepared and transferred into the agitated autoclave. Then an appropriate amount of conductive agents was added under continuous stirring until well blended. Last, the $LiFePO_4$ powders were added under constant stirring to obtain a homogeneous slurry with composition of 80 wt% active materials, 10 wt% conductive agents (unitary or binary), and 10 wt% PVDF. The solid content of the cathode slurry was controlled to be around 48 wt% to ensure the slurry viscosity of about 8,000 mPa s.

Then the cathodes were fabricated by compressing the as-prepared slurry onto an aluminum foil current collector followed by drying at 80°C in air for 24 h and 120°C in vacuum for 12 h. The electrode film was then compacted and punched into disks with a diameter of 10 mm for the half-cell assembly. Note that the $LiFePO_4$ cathode prepared with x% CNTs and y% GN was named as CNT-GN-x:y.

2.3 Cell assembly

Coin-type (CR 2032) half-cells were assembled in an argon-filled glove box, using the as-prepared $LiFePO_4$

electrode plate as a working electrode and lithium foil as a counter electrode. A Celgard-2400 microporous membrane was used to separate two electrodes. A 1-mol/L solution of $LiPF_6$ dissolved in EC/DMC (1:1, v/v) was used as the electrolyte.

2.4 Electrochemical testing

After assembly, the cells were stored and aged for 12 h before the electrochemical tests. The galvanostatic charge and discharge measurements were performed using a LAND CT2001A battery testing system with the voltage window between 2.5 and 3.7 V vs Li^+/Li. Cyclic voltammetry (CV) studies were conducted by PARSTAT 4000A electrochemical workstation at a scan rate of 1 mV s^{-1} in the voltage range of 2.5–4.2 V. Conductivity tests were carried out on a four-point probe resistivity tester (ST2258B-F02, Beijing Bolun JingWei Tech Dev Co. Ltd) using a four-point probe method by coating $LiFePO_4$ cathode slurry onto polyethylene terephthalate. All electrochemical tests were performed at room temperature.

2.5 Materials characterization

X-ray diffraction (XRD) patterns were recorded using a D8 Advance diffractometer (Bruker, Germany) equipped with a Cu-Kα radiation source. Scanning electron microscope (SEM) images were taken on an SU-8010 field emission SEM (Hitachi, Japan). The slurry apparent viscosity was measured by an MSK-SFM-VT precision digital viscometer (HF-Kejing, China).

3 Results and discussion

3.1 Raw materials characterization

The powder XRD patterns of $LiFePO_4$, SP, CNT, and GN are given in Figure 1. As shown in Figure 1a, all the intense peaks could be readily indexed to a well-crystallized $LiFePO_4$ (JCPDS card No. 40-1499), with an orthorhombic olivine structure. Two broad (002 and 001) peaks of SP revealed its poor crystallinity. In contrast,

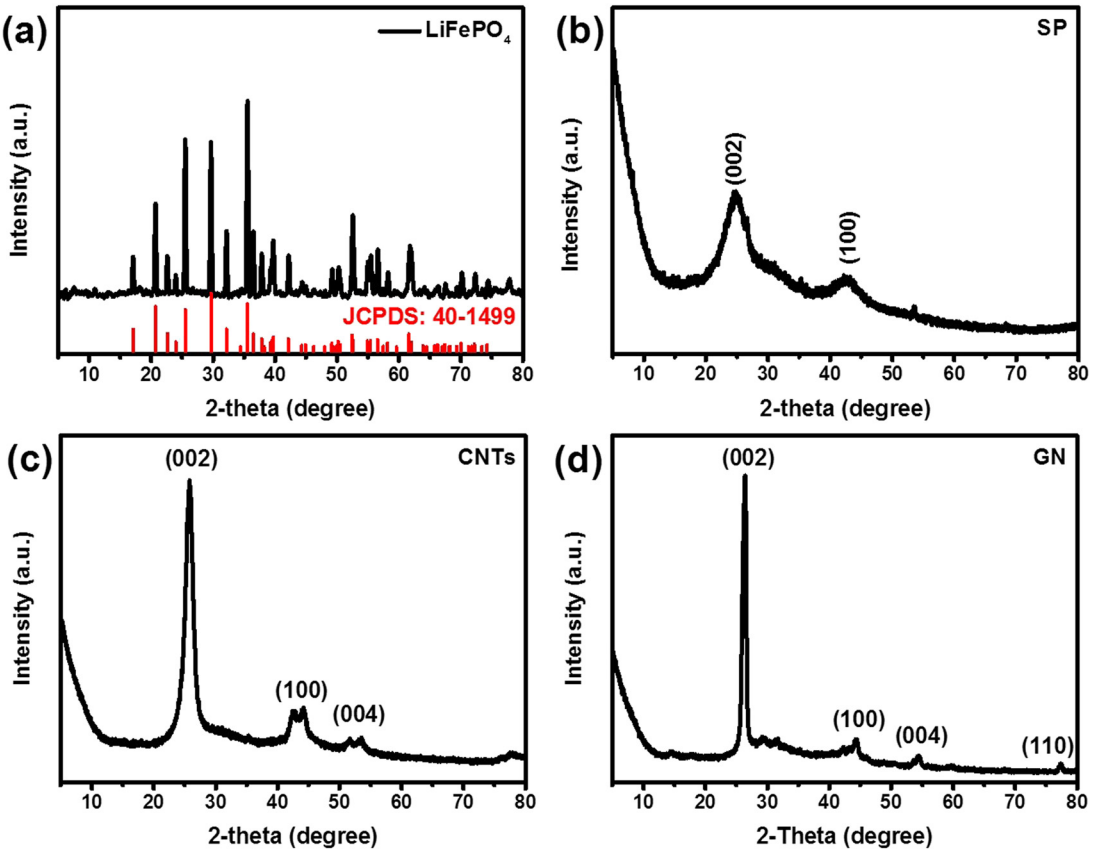

Figure 1: XRD patterns of $LiFePO_4$ (a), SP (b), CNTs (c), and GN (d).

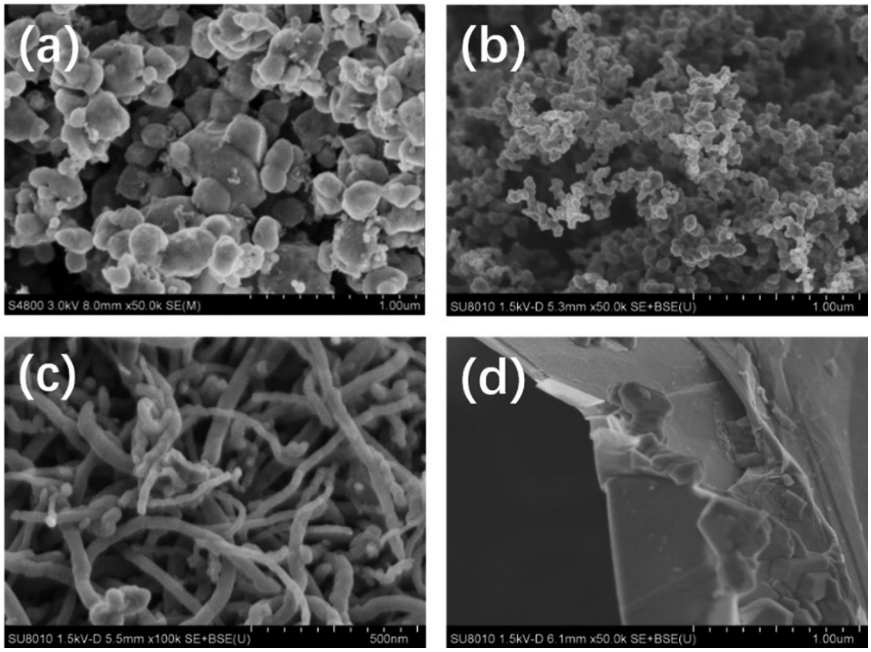

Figure 2: SEM images of $LiFePO_4$ (a), SP (b), CNTs (c), and GN (d).

the narrower (002) peak and indistinct (100 and 004) peaks of CNTs and GN indicated their higher crystallinity compared to that of SP. And there was no impurity in all three carbon-based conductive agents.

The morphology and microstructures of $LiFePO_4$, SP, CNTs, and GN are shown in Figure 2. Most $LiFePO_4$ nanoparticles were homogeneously distributed nanospheres with an average diameter of 100–200 nm (Figure 2a). Apart from their difference in crystallinity, SP, CNTs, and GN also showed varied morphological features. Specifically, SP consisted of uniformed nanoparticles with sizes ranging from 20 to 40 nm, which were smaller than that of $LiFePO_4$ nanoparticles (Figure 2b). The CNTs presented bended and entangled cylindrical tubes with an aspect ratio of about 1:1,000 (Figure 2c), while the GN exhibited a crumpled, sheet-like structure with smooth surface (Figure 2d).

3.2 Electrode characterization

Figure 3 shows the surface SEM images of the $LiFePO_4$ cathode plates with different unitary conductive agents. As shown in Figure 3a, the smaller SP particles could easily fall into the interspace between the larger $LiFePO_4$ grains and were very difficult to link up with each other [30]. As a result, the conductive paths in the cathodes are interrupted. By contrary, in cathodes with CNTs or GN, the conductive agents could easily form continuous conductive networks. In Figure 3b, the long wire-like CNTs connected with multiple $LiFePO_4$ particles and uniformly extended throughout the composite cathode without any obvious entanglement. In Figure 3c, the surface of individual fully exfoliated GN nanosheet was decorated by evenly dispersed $LiFePO_4$ particles, which could facilitate electron transfer across the surface of $LiFePO_4$ particles in short range, and ensured high utilization of GN, efficient long-range conductivity as well as sufficient contact between electrolyte and active materials [35]. Accordingly, it is promising to achieve high conductivity of the cathode with such continuous 2D conductive networks.

The surface SEM images of the $LiFePO_4$ cathode plates with various binary conductive agents in different raw material ratios are shown in Figure 4. Figure 4a1–a3 consists of the SEM images of the cathodes prepared with SP/GN in ratios of 7:3, 5:5, and 3:7, respectively. In Figure 4a1, the conductive network in $LiFePO_4$ electrode was mostly composed of SP particles due to the low content of GN. While in Figure 4a2–a3, both SP and GN particles were dispersed well among active material particles in $LiFePO_4$ cathode, suggesting the formation of an effective electronic conducting network. Figure 4b1–b3 shows the SEM images of the cathodes prepared with SP/CNT in ratios of 7:3, 5:5, and 3:7, respectively. When the content of CNTs was 3% (Figure 4b1), active

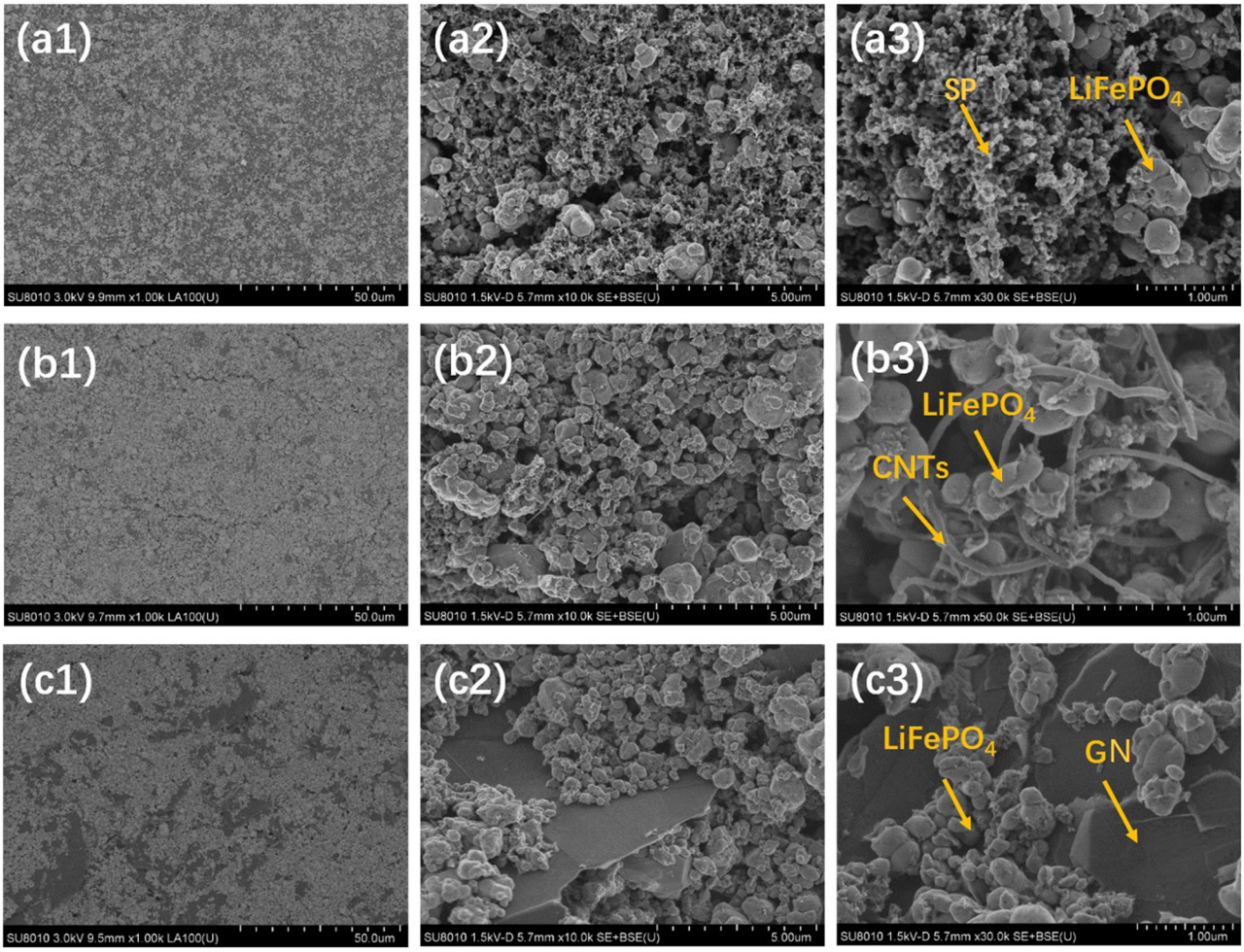

Figure 3: Surface SEM morphology of $LiFePO_4$ cathode plates with different unitary conductive agents (a1–a3: SP, b1–b3: CNT, c1–c3: GN).

material particles were uniformly dispersed, and CNTs interpenetrated between SP and active material particles to form a conductive network, which was promising to achieve high conductivity (Figure 4b1). By gradually increasing the content of CNTs, obvious entanglement of CNTs could be observed, which resulted in an agglomeration and isolation of the active material particles (Figure 4b2 and b3) [52]. The cathodes prepared with both CNTs and GN presented a very distinctive morphology (Figure 4c1–c3). Obvious agglomeration of active material particles was observed (marked in Figure 4c2 and c3), and this phenomenon was getting worse with an increase in CNT addition. As the content of CNTs was increased to 7% (Figure 4c1), the CNTs became invisible due to their self-entanglement and agglomeration of the active material particles (the inserted SEM); while large GN sheets could be clearly observed.

3.3 Electrochemical performance

Figure 5 shows the electrochemical behavior of the $LiFePO_4$ cathodes with unitary conductive agent. Typical charges/discharge profiles of the $LiFePO_4$ cathodes at 1 C between 2.5 and 3.7 V are presented in Figure 5a. It could be seen that the initial charge and discharge profiles of the three $LiFePO_4$ cathodes were almost the same and no obvious polarization was observed, delivering discharge/charge capacities of 131.8/130.7, 140.1/138.1, and 149.8/147.5 mA h g^{-1}, respectively. Obviously, the $LiFePO_4$ cathode with GN as conductive additive displayed the highest specific capacity, which could be attributed to its long-range electron conduction and large specific surface area. By contrary, SP conductive agent demonstrated low electrical conductivity and local electron conduction, thus its corresponding $LiFePO_4$ cathode displayed the lowest specific capacity among the three [53].

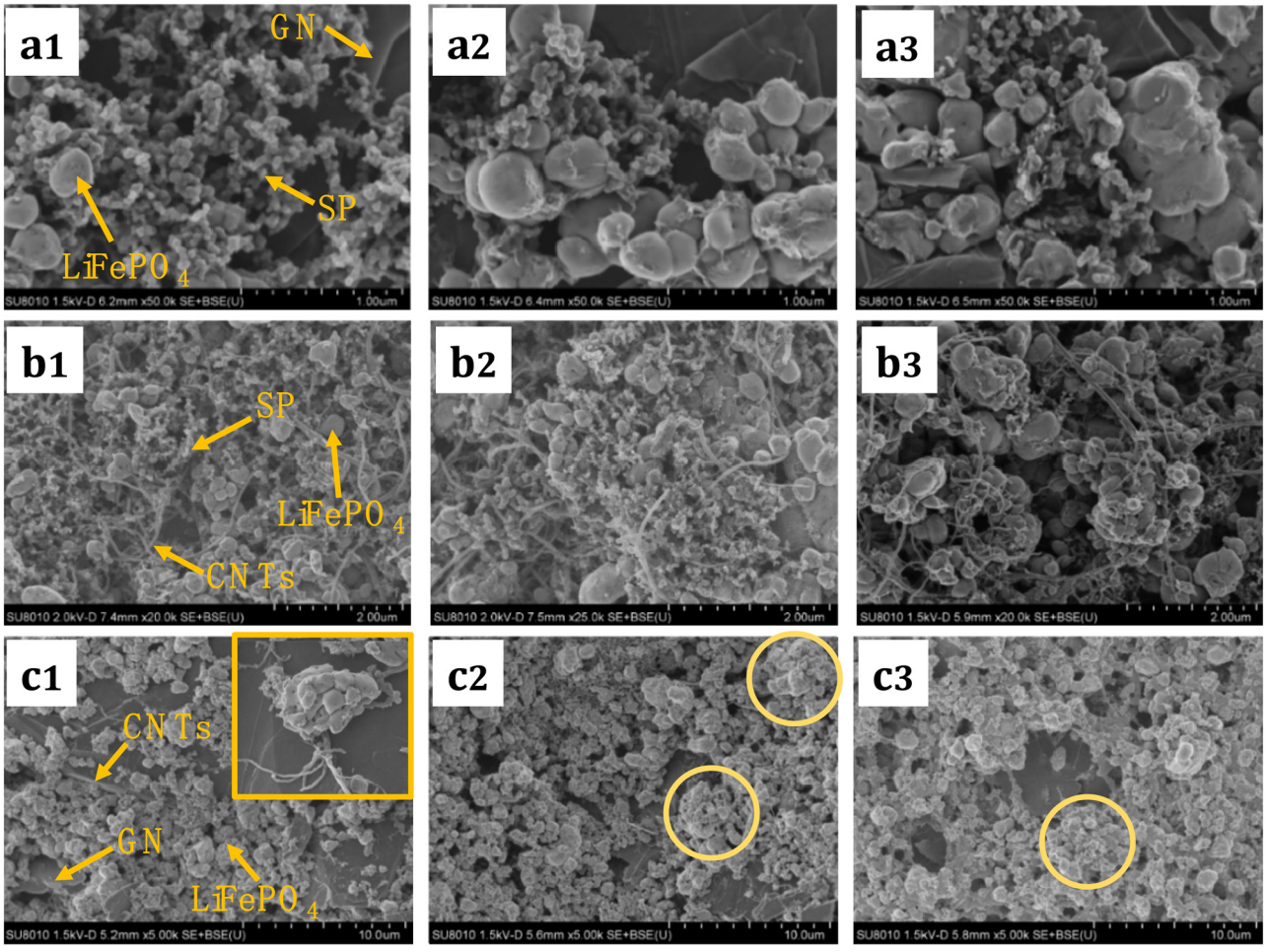

Figure 4: Surface SEM morphology of the $LiFePO_4$ cathode plates with various binary conductive agents in different ratios (a1–a3: SP-GN, b1–b3: SP-CNT, c1–c3: CNT-GN).

CV was performed in order to investigate the effect of the conductive agent on the electrochemical properties of the $LiFePO_4$ cathodes at 0.1 mV s^{-1} between 2.5 and 4.2 V. Figure 5b–d shows the initial three CV of the $LiFePO_4$ cathodes with SP, CNTs, and GN conductive agents, respectively. One pair of well-separated anodic/cathodic peaks was discovered in all CV curves, which coincided well with the results of voltage profiles in Figure 5a. Besides, the anodic/cathodic peaks of the $LiFePO_4$ cathode with GN were more symmetrical and sharper, indicating its better electrochemical activity [40]. Furthermore, the redox pairs of the $LiFePO_4$ cathode with GN exhibited the minimum potential separation (0.3 V) among the three. Therefore, with the well-defined peaks and small peak potential separation, the $LiFePO_4$ cathode with GN conductive agent could achieve good electrochemical performance.

Figure 5e compares the cycling properties of the resulted electrodes at 1 C. The capacity values of all electrodes exhibited a remarkable increase in the first 25 cycles, which then became stable, keeping 127.5, 137.9, and 141.8 mA h g^{-1} after 200 cycles. The initial capacity increases could be related to the electrode activation process. As expected, the $LiFePO_4$ cathode with GN showed both higher capacity and better cycling stability than that of the other. Moreover, when the current density increased stepwise from 0.2 to 5 C and returns to 0.2 C, a high reversible capacity (142.5 mA h g^{-1}) and a high capacity retention (99.5%) could be achieved for the GN electrode (Figure 5f).

To figure out the synergy between two different conductive agents, we examined the galvanostatic charge/discharge properties of a series of $LiFePO_4$ cathodes with varied compositions (Figure 6). Figure 6a compares the charge/discharge profiles of the $LiFePO_4$ cathodes with different binary conductive agents in the same ratio. The similar charge and discharge profiles of all electrodes indicated similar electrochemical behavior

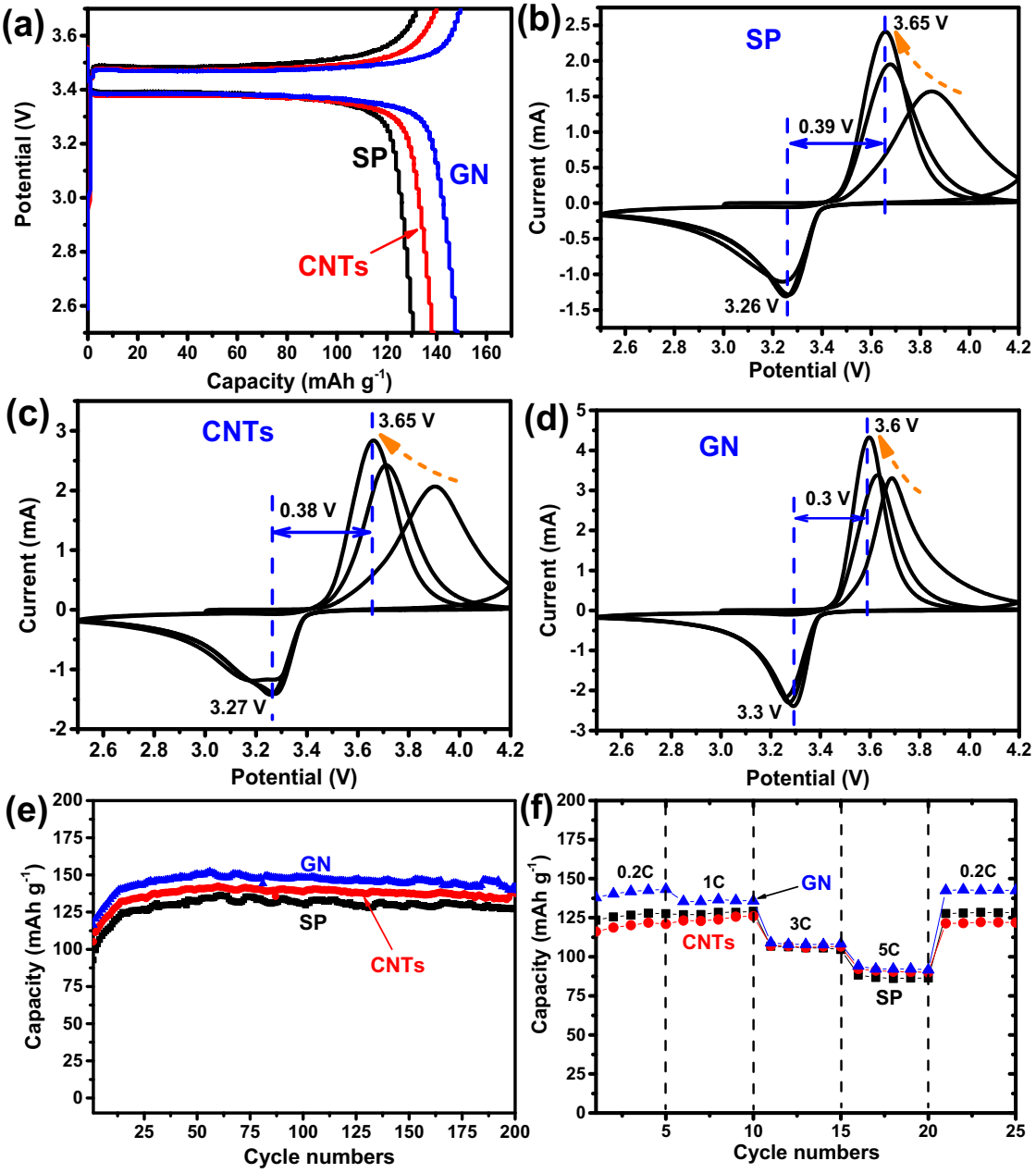

Figure 5: Electrochemical behavior of the $LiFePO_4$ cathodes with different unitary conductive agents: (a) charge/discharge profiles at 1 C; (b–d) CV curves; (e) cycling performance at 1 C; and (f) rate performance.

of the $LiFePO_4$ cathodes with different binary conductive agents. And SP-GN-5:5 electrode exhibited higher reversible capacities (151.2 mA h g^{-1}) than that of SP-CNT-5:5 (138.1 mA h g^{-1}) and CNT-GN-5:5 electrodes (115 mA h g^{-1}).

Figure 6b–d presents the effect of the ratio of binary conductive agents on the charge/discharge property of the $LiFePO_4$ cathodes. In SP-CNT binary systems, the capacity of the electrodes showed negligible improvement by increasing the content of CNTs (Figure 6b). However, a large number of curled CNTs could be entangled with each other when combined with GN, which adversely affected the dispersion of the active materials, and resulted in poor electrode performance. Therefore, the electrode capacity decreased with an increase in CNT content (Figure 6d). In addition, both SP-GN electrode (0.08 V) and CNT-GN electrode (0.07 V) exhibited smaller potential difference than that of SP-CNT electrode (0.08 V), which could be attributed to the excellent electrical conductivity and effective "plane-to-

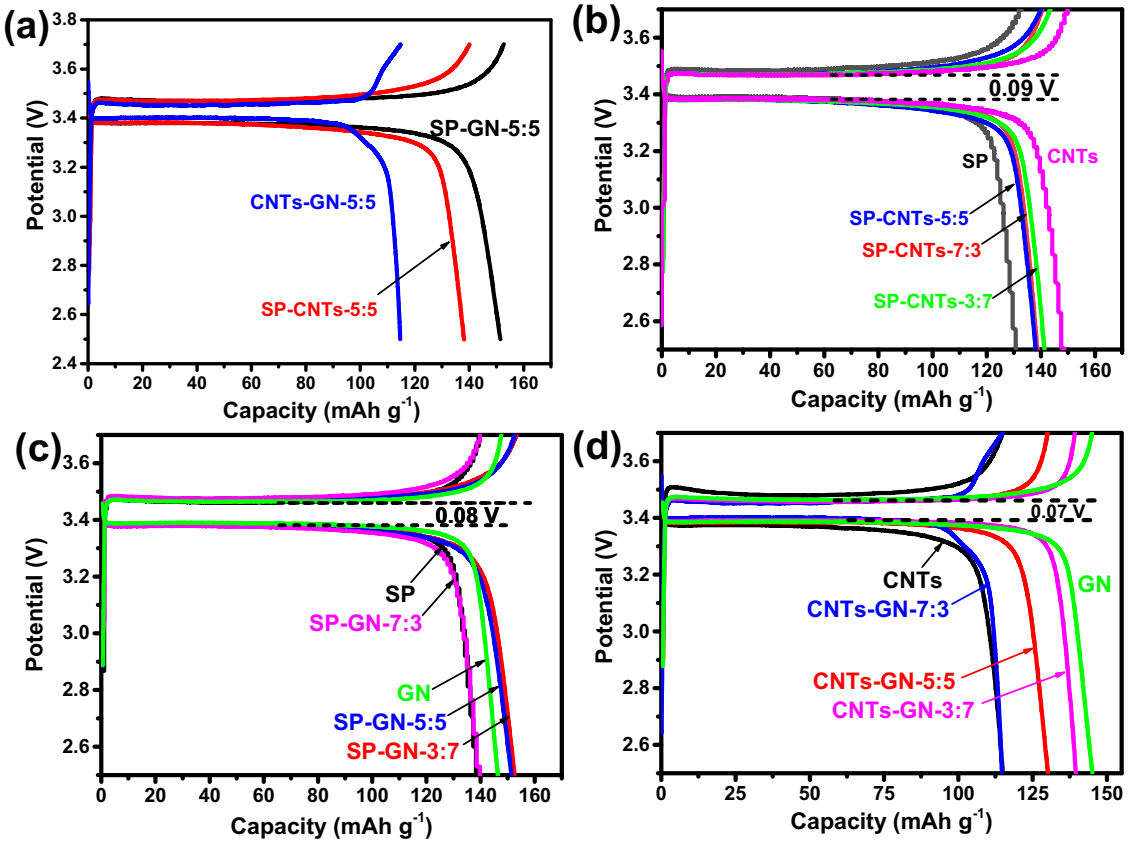

Figure 6: Typical galvanostatic charge/discharge profiles of the $LiFePO_4$ electrodes with (a–d) various binary conductive agents in different ratios at 1 C between 2.5 and 3.7 V.

point" conducting mode of GN [34,35]. The results indicated that CNTs exert a great effect on the electrode capacity and GN can effectively improve the conductivity of $LiFePO_4$ cathodes.

The cycling performance and rate capability of the $LiFePO_4$ cathodes with different binary conductive compositions are shown in Figure 7. It can be found that the electrodes with binary conductive agents displayed better electrochemical performance than those with SP only, while the electrodes with the CNT-GN combination achieved both high capacity and good cycling stability (Figure 7a–c), which may be related to their respective merits and the synergistic effect [38,54]. Based on Figure 7b, as expected, the electrode with 5% GN (SP-GN-5:5) showed the highest reversible capacity, but the electrode capacity dropped sharply with further increase in the GN content (SP-GN-3:7), probably due to the steric effect from the large planar structure of GN nanosheets [55]. On the other hand, excessive GN may cause re-stacking of GN nanosheets, which is unfavorable for smooth Li^+ diffusion. Furthermore, from Figure 7a and c, the capacity of the electrode containing 3% CNTs (SP-CNTs-7:3 and CNTs-GN-3:7) was obviously higher than that with 7% CNTs (SP-CNTs-3:7 and CNTs-GN-7:3). This means that adding excess CNTs does not benefit the electrochemical performance of the electrode, which was consistent with the aforementioned results. The rate performances of the electrodes with different binary conductive agents in the same ratio are compared in Figure 7d. All electrodes with binary conductive agents exhibited stable capacity and high capacity retention at various current densities. The low capacity of SP-GN-5:5 electrode at 0.2 C may be related to its slow electrode activation process.

The conductivity test results of $LiFePO_4$ cathodes with different binary conductive agents are shown in Figure 8. It can be found that the electrical conductivity improved with an increase in the CNT or GN content. SP-CNT cathodes with 3%, 5%, and 7% CNTs exhibited electrical conductivities of 73.8, 104.9, and 144.1 mS mm^{-1} (Figure 8a), respectively; while the cathodes employing SP-GN displayed electrical conductivities of 87.9 mS mm^{-1} (3%), 161.8 mS mm^{-1} (5%), and 247.4 mS mm^{-1} (7%; Figure 8b), respectively. Obviously, the

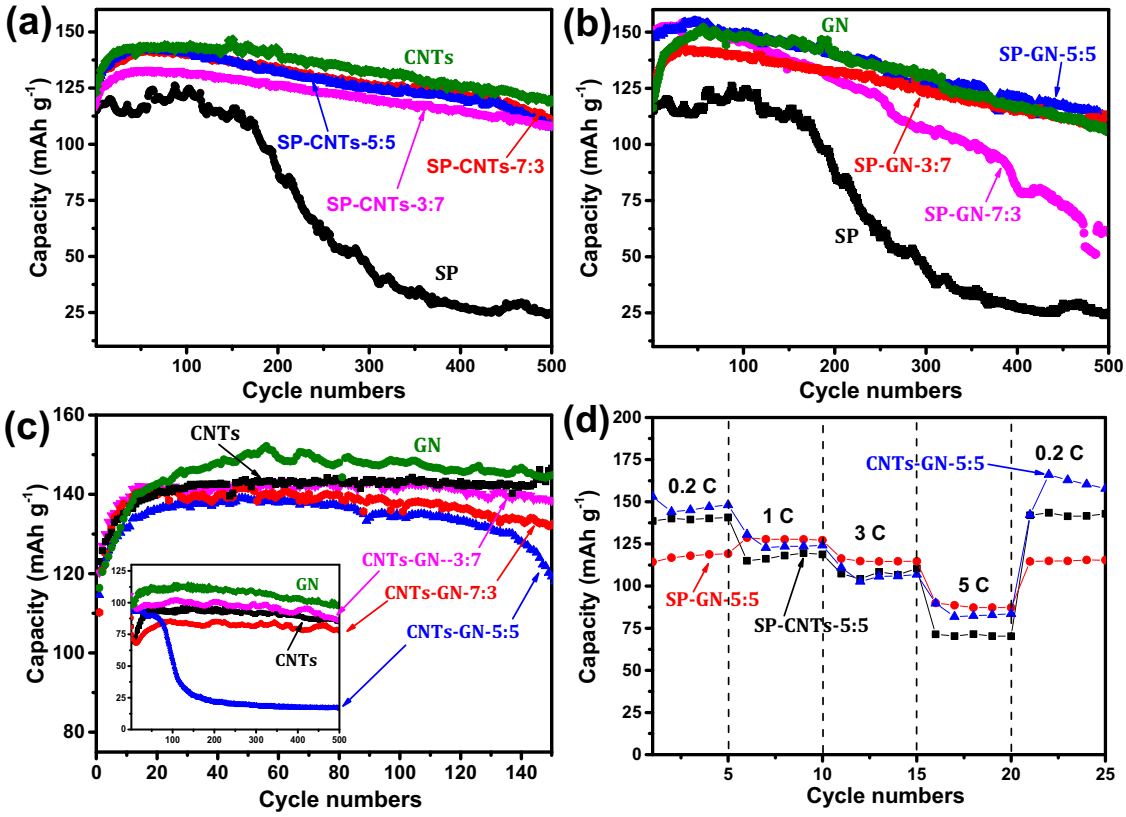

Figure 7: Electrochemical behavior of the $LiFePO_4$ cathodes with different binary conductive agents: (a–c) cycling performance at 1 C (the inset is the cycling performance at 5 C); and (d) rate performance.

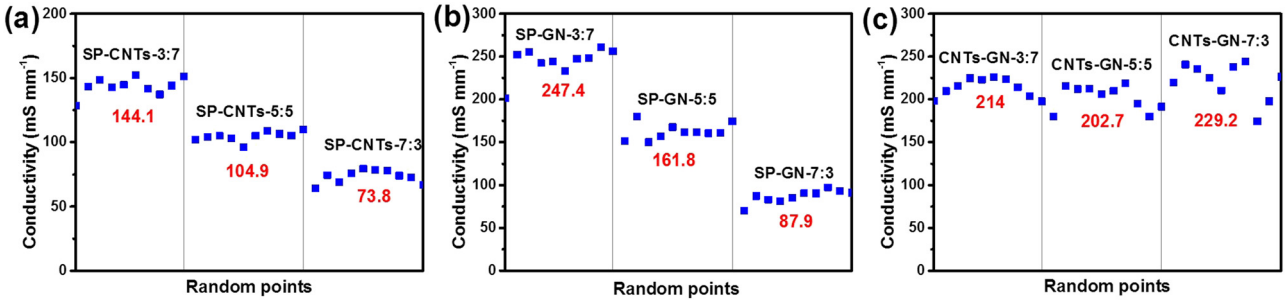

Figure 8: The electrical conductivity plots of the $LiFePO_4$ cathodes with different binary conductive agents: (a) SP-CNT, (b) SP-GN, and (c) CNT-GN.

electrical conductivities of the electrode containing GN were higher than that of the electrode with CNTs, which could be attributed to the higher electrical conductivity of GN than that of CNTs. In addition, the electrodes containing both CNTs and GN exhibited high and stable electrical conductivities, resulting from their excellent conductivity and the synergistic effect originating from the 3D conductive network constructed by CNT nanowire and GN nanosheets (Figure 8c). It should be noted that the electrical conductivity fluctuated significantly when the content of the CNTs increased to 7% (Figure 8a and c), indicating a heterogeneous distribution of the conductive network, which was directly reflected in the decreased electrochemical performance of the electrodes. All these results corresponded well with the SEM and electrochemical test results.

4 Conclusions

In summary, binary conductive agents were made by adding suitable amount of commercial CNTs and/or GN to SP to improve the conductivity of the $LiFePO_4$ cathodes in LIBs. The impact of single conductive agent and the binary conductive agents on the electrochemical performance of the $LiFePO_4$ cathodes was inspected. Meanwhile, the effect of the ratio of binary conductive agents on the properties of the $LiFePO_4$ cathode was also investigated. Results indicated that the binary conductive agents can provide more effective conductive network and faster Li^+ transport compared to traditional cathode system (only SP used). Especially, the electrode prepared with CNTs and GN as binary conductive agents exhibited both high capacity and good cycling stability. The best electrochemical performance of the cathode was obtained with the combination of 3% CNTs and 7% GN. Therefore, the binary conductive agents consisting of CNTs and GN present a promising candidate for devising high-performance $LiFePO_4$ cathodes. Such facile and scalable preparation procedure could be extended to various prospective electrode materials.

Acknowledgments: This work was supported by the National Natural Science Foundation of China (21503282) and the Fundamental Research Funds for the Central Universities (CZP19001).

Conflict of interest: The authors declare no conflicts of interest regarding the publication of this paper.

References

[1] Kang B, Ceder G. Battery materials for ultrafast charging and discharging. Nature. 2009;458(7235):190–3.
[2] Goodenough JB, Kim Y. Challenges for rechargeable Li batteries. Chem Mater. 2010;22(3):587–603.
[3] Dunn B, Kamath H, Tarascon JM. Electrical energy storage for the grid: a battery of choices. Science. 2011;334(6058):928–35.
[4] Zhou HS. New energy storage devices for post lithium-ion batteries. Energy Environ Sci. 2013;6(8):2256.
[5] Goodenough JB, Park KS. The Li-ion rechargeable battery: a perspective. J Am Chem Soc. 2013;135(4):1167–76.
[6] Wang FX, Wu XW, Li CY, Zhu YS, Fu LJ, Wu YP, et al. Nanostructured positive electrode materials for post-lithium ion batteries. Energy Environ Sci. 2016;9(12):3570-611.
[7] Sari HMK, Li XF. Controllable cathode-electrolyte interface of $Li[Ni_{0.8}Co_{0.1}Mn_{0.1}]O_2$ for lithium ion batteries: a review. Adv Energy Mater. 2019;9(39):1901597.
[8] Liu ZC, Yuan XH, Zhang SS, Wang J, Huang QH, Yu NF, et al. Three-dimensional ordered porous electrode materials for electrochemical energy storage. NPG Asia Mater. 2019;11:12.
[9] Zhang XH, Zou LF, Xu YB, Cao X, Engelhard MH, Matthews BE, et al. Advanced electrolytes for fast-charging high-voltage lithium-ion batteries in wide-temperature range. Adv Energy Mater. 2020;10(22):2000368.
[10] Wang HW, Fu JZ, Wang C, Wang JY, Yang AK, Li CC, et al. A binder-free high silicon content flexible anode for Li-ion batteries. Energy Environ Sci. 2020;13(3):848–58.
[11] Kang B, Ceder G. Battery materials for ultrafast charging and discharging. Nature. 2009;458(7235):190–3.
[12] Wang YG, He P, Zhou HS. Olivine $LiFePO_4$: development and future. Energy Environ Sci. 2011;4(3):805–17.
[13] Yuan LX, Wang ZH, Zhang WX, Hu XL, Chen JT, Huang YH, et al. Development and challenges of $LiFePO_4$ cathode material for lithium-ion batteries. Energy Environ Sci. 2011;4(2):269–84.
[14] Zhu CB, Yu Y, Gu L, Weichert K, Maier J. Electrospinning of highly electroactive carbon-coated single-crystalline $LiFePO_4$ nanowires. Angew Chem Int Ed. 2011;50(28):6278–82.
[15] Zhao Y, Peng LL, Liu BR, Yu GH. Single-crystalline $LiFePO_4$ nanosheets for high-rate Li-ion batteries. Nano Lett. 2014;14(5):2849–53.
[16] Mathew V, Alfaruqi MH, Gim J, Song JJ, Kim SJ, Ahn D, et al. Morphology-controlled $LiFePO_4$ cathodes by a simple polyol reaction for Li-ion batteries. Mater Charact. 2014;89:93–101.
[17] Wang JJ, Sun XL. Olivine $LiFePO_4$: the remaining challenges for future energy storage. Energy Environ Sci. 2015;8(4):1110–38.
[18] Guo XL, Lan T, Zhang L, Tan JW, Feng X, Li D, et al. A stable filamentous coaxial microelectrode for Li-ion batteries: a case of olivine $LiFePO_4$. Chem Commun. 2019;55(24):3529–31.
[19] Patil V, Oh W, Yoo JW, Pu L, Park JH, Yoon WS, et al. Carbon-coated supraballs of randomly packed $LiFePO_4$ nanoplates for high rate and stable cycling of Li-ion batteries. Part Part Syst Charact. 2019;36(7):1900149.
[20] Duan WY, Zhao MS, Mizuta Y, Li YL, Xu T, Wang F, et al. Superior electrochemical performance of a novel $LiFePO_4$/C/CNTs composite for aqueous rechargeable lithium-ion batteries. Phys Chem Chem Phys. 2020;22(4):1953–62.
[21] Chung SY, Chiang YM. Microscale measurements of the electrical conductivity of doped $LiFePO_4$. Electrochem Solid-State Lett. 2003;6(12):A278–81.
[22] Shi SQ, Liu LJ, Ouyang CY, Wang DS, Wang ZX, Chen LQ, et al. Enhancement of electronic conductivity of $LiFePO_4$ by Cr doping and its identification by first-principles calculations. Phys Rev B. 2003;68(19):195108.
[23] Herle PS, Ellis B, Coombs N, Nazar LF. Nano-network electronic conduction in iron and nickel olivine phosphates. Nat Mater. 2004;3:147–52.
[24] Xu YN, Chung SY, Bloking JT, Chiang YM, Ching WY. Electronic structure and electrical conductivity of undoped $LiFePO_4$. Electrochem Solid-State Lett. 2004;7(6):A131–4.
[25] Jin B, Jin EM, Park KH, Gu HB. Electrochemical properties of $LiFePO_4$-multiwalled carbon nanotubes composite cathode

materials for lithium polymer battery. Electrochem commun. 2008;10(10):1537–40.
[26] Prosini PP, Lisi M, Zane D, Pasquali M. Determination of the chemical diffusion coefficient of lithium in $LiFePO_4$. Solid State Ionics. 2002;148(1–2):45–51.
[27] Padhi AK, Nanjundaswamy KS, Goodenough JB. Phospho-olivines as positive-electrode materials for rechargeable lithium batteries. J Electrochem Soc. 1997;144(4):1188–94.
[28] Whittingham MS. Lithium batteries and cathode materials. Chem Rev. 2004;104:4271–301.
[29] Kapaev RR, Novikova SA, Chekannikov AA, Gryzlov DY, Kulova TL, Skundin AM, et al. Effect of carbon sources and synthesis conditions on the $LiFePO_4$/C cathode properties. Rev Adv Mater Sci. 2018;57(2):183–92.
[30] Dominko R, Gaberscek M, Drofenik J, Bele M, Pejovnik S, Jamnik J. The role of carbon black distribution in cathodes for Li ion batteries. J Power Sources. 2003;119–121:770–3.
[31] Wang K, Wu Y, Luo S, He XF, Wang JP, Jiang KL, et al. Hybrid super-aligned carbon nanotube/carbon black conductive networks: a strategy to improve both electrical conductivity and capacity for lithium ion batteries. J Power Sources. 2013;233:209–15.
[32] Song H, Oh Y, Çakmakçı N, Jeong Y. Effects of the aspect ratio of the conductive agent on the kinetic properties of lithium ion batteries. RSC Adv. 2019;9(70):40883–6.
[33] Liu YF, Jiang LY, Wang HN, Wang H, Jiao W, Chen GZ, et al. A brief review for fluorinated carbon: synthesis, properties and applications. Nanotechnol Rev. 2019;8(1):573–86.
[34] Su FY, You CH, He YB, Lv W, Cui W, Jin FM, et al. Flexible and planar graphene conductive additives for lithium-ion batteries. J Mater Chem. 2010;20(43):9644–50.
[35] Su FY, He YB, Li BH, Chen XC, You CH, Wei W, et al. Could graphene construct an effective conducting network in a high-power lithium ion battery? Nano Energy. 2012;1(3):429–39.
[36] Li ZH, Xu K, Pan YS. Recent development of supercapacitor electrode based on carbon materials. Nanotechnol Rev. 2019;8(1):35–49.
[37] Ghouri ZK, Motlak M, Afaq S, Barakat NAM, Abdala A. Template-free synthesis of Se-nanorods-rGO nanocomposite for application in supercapacitors. Nanotechnol Rev. 2019;8(1):661–70.
[38] Wen LZ, Sun JC, An LW, Wang XY, Ren X, Liang GC. Effect of conductive material morphology on spherical lithium iron phosphate. Nanomaterials. 2018;8(11):904.
[39] Pan YS, Xu K, Wu CL. Recent progress in supercapacitors based on the advanced carbon electrodes. Nanotechnol Rev. 2019;8(1):299–314.
[40] Wang L, Wang HB, Liu ZH, Xiao C, Dong SM, Han PX, et al. A facile method of preparing mixed conducting LiFePO4/graphene composites for lithium-ion batteries. Solid State Ionics. 2010;181(37–38):1685–9.
[41] Glukharev AG, Konakov VG. Synthesis and properties of zirconia-graphene composite ceramics: a brief review. Rev Adv Mater Sci. 2018;56(1):124–38.
[42] Konakov VG, Kurapova OY, Solovyeva EN, Lomakin IV, Archakov IY. Synthesis, structure and mechanical properties of bulk "copper-graphene" composites. Rev Adv Mater Sci. 2018;57(2):151–7.
[43] Wei XF, Guan YB, Zheng XH, Zhu QZ, Shen JR, Qiao N, et al. Improvement on high rate performance of $LiFePO_4$ cathodes using graphene as a conductive agent. Appl Surf Sci. 2018;440:748–54.
[44] Han XY, Li R, Qiu SQ, Zhang XF, Zhang Q, Yang YK. Sonochemistry-enabled uniform coupling of SnO_2 nanocrystals with graphene sheets as anode materials for lithium-ion batteries. RSC Adv. 2019;9(11):5942–7.
[45] Huang ZY, Han XY, Cui X, He CG, Zhang JL, Wang XG, et al. Vertically aligned VS_2 on graphene as a 3D heteroarchitectured anode material with capacitance-dominated lithium storage. J Mater Chem A. 2020;8(12):5882–9.
[46] Bobylev SV, Sheinerman AG. Effect of crack bridging on the toughening of ceramic/graphene composites. Rev Adv Mater Sci. 2018;57(1):54–62.
[47] Zhu LB, Xu JW, Xiu YH, Sun YY, Hess DW, Wong CP. Growth and electrical characterization of high-aspect-ratio carbon nanotube arrays. Carbon. 2006;44(2):253–8.
[48] Hashim H, Salleh MS, Omar MZ. Homogenous dispersion and interfacial bonding of carbon nanotube reinforced with aluminum matrix composite: a review. Rev Adv Mater Sci. 2019;58(1):295–303.
[49] Gao Y, Jing HW, Zhou ZF. Fractal analysis of pore structures in graphene oxide-carbon nanotube based cementitious pastes under different ultrasonication. Nanotechnol Rev. 2019;8(1):107–15.
[50] Huynh LTN, Tran TTD, Nguyen HHA, Nguyen TTT, Tran VM, Grag A, et al. Carbon-coated $LiFePO_4$-carbon nanotube electrodes for high-rate Li-ion battery. J Solid State Electrochem. 2018;22(7):2247–54.
[51] Ventrapragada LK, Creager SE, Rao AM, Podila R. Carbon nanotubes coated paper as current collectors for secondary Li-ion batteries. Nanotechnol Rev. 2019;8(1):18–23.
[52] Sotowa C, Origi G, Takeuchi M, Nishimura Y, Takeuchi K, Jang IY, et al. The reinforcing effect of combined carbon nanotubes and acetylene blacks on the positive electrode of lithium-ion batteries. ChemSusChem. 2008;1(11):911–5.
[53] Liu G, Zheng H, Simens AS, Minor AM, Song X, Battaglia VS. Optimization of acetylene black conductive additive and PVDF composition for high-power rechargeable lithium-ion cells. J Electrochem Soc. 2007;154(12):A1129–34.
[54] Lei XL, Zhang HY, Chen YM, Wang WG, Ye YP, Zheng CC, et al. A three-dimensional $LiFePO_4$/carbon nanotubes/graphene composite as a cathode material for lithium-ion batteries with superior high-rate performance. J Alloys Compd. 2015;626:280–6.
[55] Zhang B, Yu Y, Liu YS, Huang ZD, He YB, Kim JK. Percolation threshold of graphene nanosheets as conductive additives in $Li_4Ti_5O_{12}$ anodes of Li-ion batteries. Nanoscale. 2013;5(5):2100–6.